Fundamental electrical properties of fluorinated and N2O plasma annealed ultrathin silicon oxides grown by microwave plasma afterglow oxidation at low temperatures

P. C. Chen, Klaus Y. J. Hsu, H. L. Hwang, and J. Y. Lin

Citation: J. Appl. Phys. **76**, 5508 (1994); doi: 10.1063/1.357170

View online: http://dx.doi.org/10.1063/1.357170

View Table of Contents: http://jap.aip.org/resource/1/JAPIAU/v76/i9

Published by the American Institute of Physics.

Fundamental electrical properties of fluorinated and N_2O plasma-annealed ultrathin silicon oxides grown by microwave plasma afterglow oxidation at low temperatures

P. C. Chen, Klaus Y. J. Hsu, and H. L. Hwang
Department of Electrical Engineering, National Tsing Hua University, Hsin-chu, Taiwan 30043, Republic of China

J. Y. Lin
Department of Electrical Engineering, Chung Cheng Institute of Technology, Ta-shi, Tao-yuan, Taiwan, Republic of China

(Received 4 January 1994; accepted for publication 11 July 1994)

A technique for growing ultrathin silicon oxides of superior quality at low temperatures is indispensable for future submicron device applications. Fundamental characteristics such as the oxide breakdown fields, oxide charges, and interface-state densities of various ultrathin silicon oxides ($\leq$8 nm) grown by microwave plasma afterglow oxidation at low temperatures (400 and 600 °C) were investigated. Fluorination (HF soaking) and low-temperature N_2O plasma annealing were employed to improve the properties of the oxides. The breakdown fields of the as-grown silicon oxides were enhanced and the interface-state densities were reduced. The effect of N_2O annealing time on the interface-state density was also investigated. A longer annealing time (>1 h) was required to reduce the interface-state density. The effective oxide charge density of 600 °C as-grown oxide was as low as 6×10^{10} cm^{-2}. Additionally, the breakdown field of the thin silicon oxide grown at 600 °C with 15 min N_2O plasma annealing was 12 MV/cm.

I. INTRODUCTION

When miniaturization of ultra-large-scale integrated circuits (ULSI) entered the deep submicron domain, improvements of metal-oxide-semiconductor field-effect transistors' (MOSFETs') performance have been achieved by scaling down the gate oxide thickness to less than 10 nm. Low-temperature processes are indispensable to maintain the shallow dopant profiles as well as reduce the strain in oxide films during the thin oxide growth. The utilization of a low-temperature plasma (induced by rf or microwave) oxidation process can satisfy these requirements.[1–4] In these processes, substrates are generally introduced into the discharge region, thereby exposing the samples to the plasma, which contains high-energy particles and UV radiation. This can easily cause oxide damage. If the substrates are placed away from the plasma region, the reactive species (oxygen atoms) diffuse to the substrate mainly due to the concentration gradient and the gas flow.[5–8] Moreover, the plasma induced by microwave (2.45 GHz) contains less energetic particles than a rf (13.56 MHz) plasma (the kinetic energy of ions in a microwave plasma is less than 10 eV, which is lower than the sputter threshold of most materials). A downstream type of microwave plasma system should be adequate to grow ultrathin oxides for ULSI devices.

Oxidation kinetics of microwave plasma afterglow (downstream) oxidation have been studied in the past few years.[7–10] Although this technique is suitable for ultrathin oxide growth at low temperatures, the electrical properties of such oxides have been discussed rarely in the previous literature.[6] On the other hand, improvement in gate oxide reliability is an important issue for ULSI devices. The addition of fluorine[11–14] and N_2O gas annealing[15–18] have been demonstrated to achieve this goal by conventional high-temperature furnace techniques; however, these techniques were typically employed at very high temperatures. Especially for N_2O annealing, the temperatures were usually higher than 950 °C. In this study, microwave plasma afterglow oxidation was utilized to grow ultrathin oxides (7–8 nm) at 400 and 600 °C. The fluorine addition and the low-temperature N_2O plasma annealing were performed for the first time in such a system. Electrical properties of these ultrathin oxides were investigated. The effects of fluorine and N_2O plasma annealing were also examined. Some properties of the oxides in this study are superior to those reported previously by the same method.[6] The techniques employed in this study are potentially suitable for 0.1 μm device applications if further improvements can be made.

II. EXPERIMENT

A schematic diagram of the experimental apparatus is illustrated in Fig. 1. The furnace tube is evacuated with a mechanical pump. Microwave energy is guided through a coaxial cable into a McCarroll cavity.[19] Additionally, gases flow through a fused quartz tube located within the cavity. The plasma is initiated by a Tesla coil. Furthermore, the cavity can be tuned to the resonance frequency of the microwaves to lower the reflection power. Gas will become an atomic species after flowing out of the cavity. The quartz tube was designed to have a 90° bend to ensure that the energetic particles and UV light would not damage the samples. The samples were placed approximately 15 cm away from the plasma discharge region.

N-type, 4–7 Ω cm, (100)-oriented Si wafers were used as substrates. Oxide layers 800 nm thick were first grown thermally on Si wafers and then patterned to 5×10^{-4} cm^{-2} square holes as the capacitor regions. The samples were then

 0021-8979/94/76(9)/5508/7/$6.00

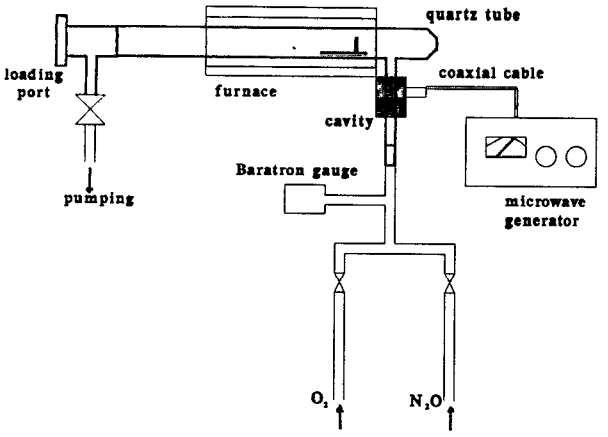

FIG. 1. The schematic diagram of the experimental apparatus.

cleaned by a modified RCA method[20] and transferred into the oxidation system to grow thin oxides. The forward microwave power was 100 W and the oxygen pressure was 1 Torr. The oxidation rate was normally around 0.12 nm/min at 600 °C.

To fabricate fluorinated oxides, RCA cleaning was followed by soaking in HF solution [de-ionized (DI) water:HF =10:1], and without DI water rinse the samples were directly loaded into the oxidation tube to grow oxides.

The N_2O plasma-annealed samples were grown at 600 °C in 1 Torr O_2 plasma to a thickness of 6.5 nm. The growth was immediately followed by a 100 W microwave annealing in 3 Torr N_2O plasma for 15, 30, and 60 min, respectively.

Next, 1 μm Al films were sputter deposited and patterned as the electrodes. The backsides of samples were also coated with Al to ensure good ohmic contacts. For obtaining the inherent electrical properties of these oxides and preventing Al from penetrating through the thin oxide films, all of the samples were annealed in pure N_2 (without H_2) gas at 250 °C for 30 min as the post-metallization anneal (PMA). This PMA was effective in reducing those charges trapped during the fabrication processes.[21]

The breakdown fields of oxides were obtained from I-V measurements. The flatband voltage V_{fb}, effective oxide charge Q_{eff}, and interface-state density D_{it} were determined from the high-frequency (100 kHz) and quasistatic capacitance-voltage (HFCV and QSCV) curves measured with a Keithley model 82 system. Additionally, the oxide thicknesses were derived from the HFCV measurements.

III. RESULTS AND DISCUSSION

The oxide thicknesses d, V_{fb}, and Q_{eff} of the as-grown and fluorinated oxides are listed in Table I. Q_{eff} includes the oxide trapped charges Q_{ot}, mobile ion charges Q_m, fixed oxide charges Q_f, and part of the interface state charges Q_{it}.[22] Q_m and Q_{ot} are low due to the RCA cleaning and the 250 °C PMA. Since the samples were not annealed in a H_2 environment, the value of D_{it} was not low enough to be neglected;[23] therefore, the Q_{eff} should mainly include Q_f and Q_{it} but it is difficult to distinguish between them. As can be seen from the relative values of V_{fb} and Q_{eff} listed in Table I, the charges Q_{eff} in the oxide grown at higher temperature (600 °C) are lower than those grown at 400 °C. Furthermore, the addition of fluorine led toward more positive charges in those oxides. This phenomenon was also observed in the NF_3 purge fluorinated experiment.[24] Since fluorine may displace oxygen by breaking the Si—O—Si bonds in forming the Si—F bonds, it was speculated that the interfacial nonbridging oxygen centers may be the origin of the positive charges.

TABLE I. Thickness, flatband voltage, and oxide charges of as-grown and fluorinated oxides.

Sample preparation conditions	Thickness (d) (nm)	V_{fb} (V)	Q_{eff} (no./cm^2)
600 °C	8	−0.35	5.8×10^{10}
400 °C	7	−0.36	8.8×10^{10}
600 °C+F	7.2	−0.37	1.9×10^{11}
400 °C+F	7	−0.39	2×10^{11}

Figure 2(a) shows the breakdown field distributions of the as-grown and fluorinated oxides. No major difference occurs in the distributions between the 600 and 400 °C as-grown oxides despite the fact that the breakdown-field distribution of the oxides grown at 400 °C is more dispersive. The breakdown field of the fluorinated oxides grown at 600 °C could be improved to 11 MV/cm; however, the breakdown fields of the fluorinated oxides grown at 400 °C were worse than those of the as-grown oxides. Figure 2(b) shows the cumulative failure rate as a function of the electric fields applied to the samples of Fig. 2(a). In view of the breakdown properties as shown in Fig. 2(b), fluorinated oxides grown at 600 °C had only a 20% failure rate at an electric field of 7 MV/cm while others had almost completely broken down. It may be that fluorine might "seal" some micropores in the oxides grown by this oxidation technique to reduce the B-mode breakdown mechanism (caused by weak spots in the oxides).[25] This sealing process appears to work only at the higher oxidation temperature (600 °C). The fluorinated oxides grown at 400 °C had inferior properties. Ma[26] showed that too much F in the oxides would deteriorate the oxide properties, and Jeng *et al.*[27] have also shown that fluorine exhibits an anomalous out-diffusion behavior in Si at a temperatures$\geqslant$550 °C. Therefore, the fluorinated oxides grown at 400 °C might contain too much F and have a poor breakdown property.

Figure 3 shows the interface-state density D_{it} of the samples listed in Table I. As illustrated in Fig. 3, D_{it} of the oxides grown at 600 °C is lower than those grown at 400 °C. Additionally, the fluorinated process can reduce D_{it} throughout the whole silicon band gap. The D_{it} at the mid-band gap D_{itm} of the fluorinated oxide grown at 400 °C was still high; however, the D_{it} near the valence-band edge was significantly reduced. Fluorine has an annealing effect on D_{it} of the oxides grown by this technique (especially near the valence-band edge), and it became more efficient at a higher temperature (600 °C). The D_{it} near band edges (band-tail states) were proposed to be induced by the presence of a thin, disordered Si layer[28] or Si-Si weak bonds[29] at the SiO_2/Si interface. The

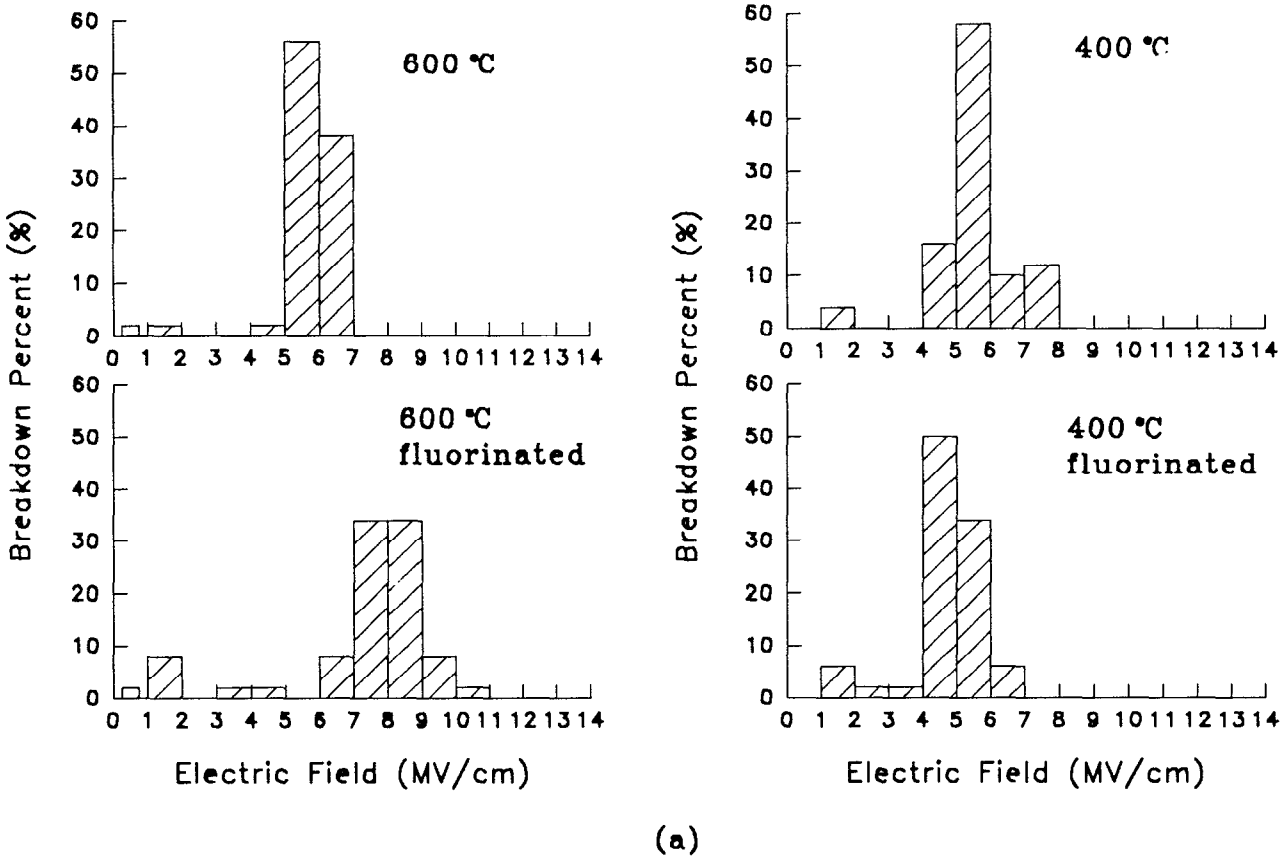

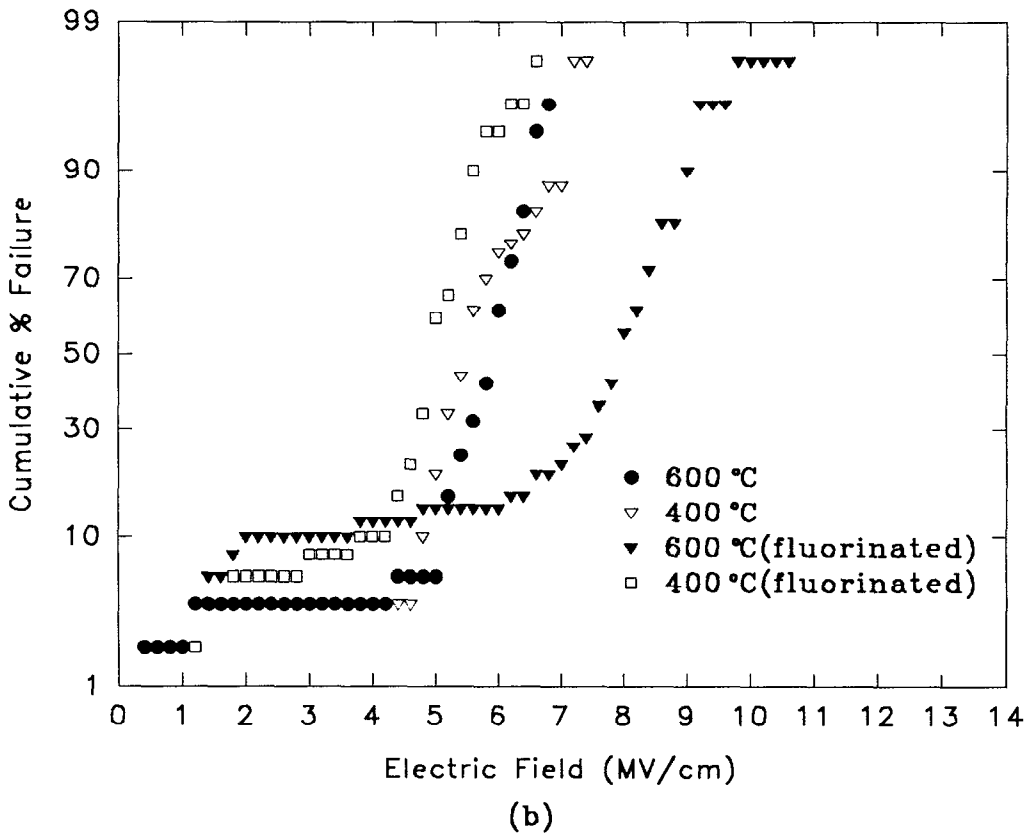

FIG. 2. The breakdown properties of the as-grown and fluorinated oxides; (a) breakdown field distributions; (b) the cumulative failure rates.

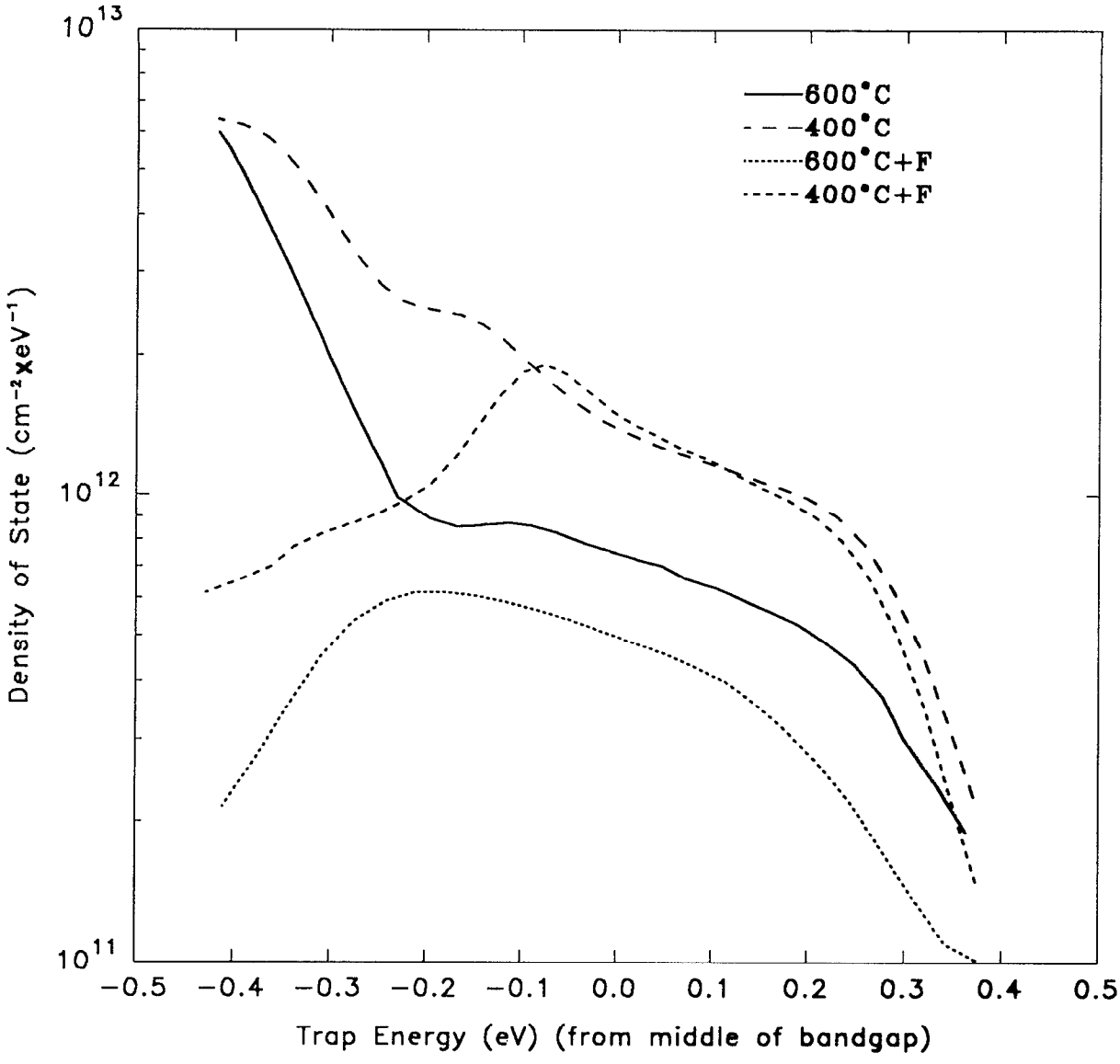

FIG. 3. The interface-state densities of the samples listed in Table I.

disordered layer causes the perturbation of states out of the Si bands into the gap, and the weak Si bonds also introduce gap states near the valence band. Fluorine appears to be effective in reducing the strained, disordered Si layers or Si weak bonds at the interface by forming Si—F bonds. The origin of D_{itm} is believed to be the Si dangling bonds at the SiO_2/Si interface.[29] It appears that fluorine atoms are more active in reducing the dangling bonds at the SiO_2/Si interface at a higher temperature. As demonstrated by the curves of Fig. 3, the D_{it} at the mid-band gap is higher than that near the conduction-band edge, and the D_{itm} of fluorinated oxides is actually higher than those near both band edges. This is in contrast to the conventional thermal oxide with a 450 °C forming gas PMA, in which the D_{it} near both band edges are higher than the D_{itm} (due to H-atom annealing the Si dangling bonds).[30]

It should be noted that the data discussed here are the inherent properties of oxides grown by microwave plasma afterglow oxidation. The D_{itm}, although higher (≈ 5–7×10^{11} $cm^{-2}\,eV^{-1}$) than the usual value for device applications, is not substantially higher than values measured in as-grown 800 °C thermal oxides.[31] Annealing them by performing the conventional 450 °C forming gas PMA is a relatively easy task.[23,31]

For the N_2O plasma-annealed samples, the annealing condition, oxide thickness, V_{fb}, and Q_{eff} are listed in Table II. N_2O plasma-annealed oxides have a higher Q_{eff} than those of the as-grown oxides. This phenomenon is similar to the

TABLE II. Thickness, flatband voltage, and oxide charges of 600 °C 3 Torr N_2O plasma annealing oxides.

N_2O annealing time (min)	Thickness (d) (nm)	V_{fb} (V)	Q_{eff} (no./cm^2)
15	6.7	−0.44	3.9×10^{11}
30	7.7	−0.44	3.3×10^{11}
60	8	−0.47	3.8×10^{11}

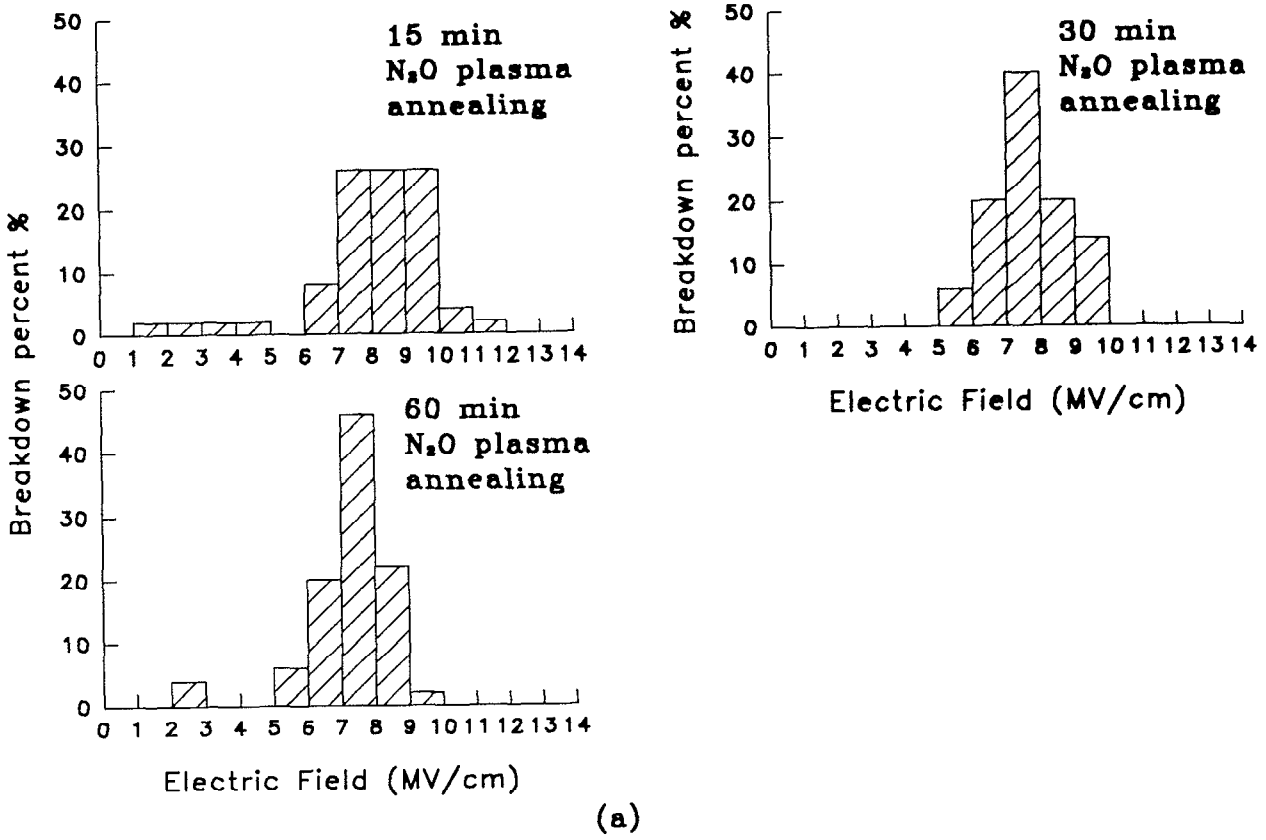

(a)

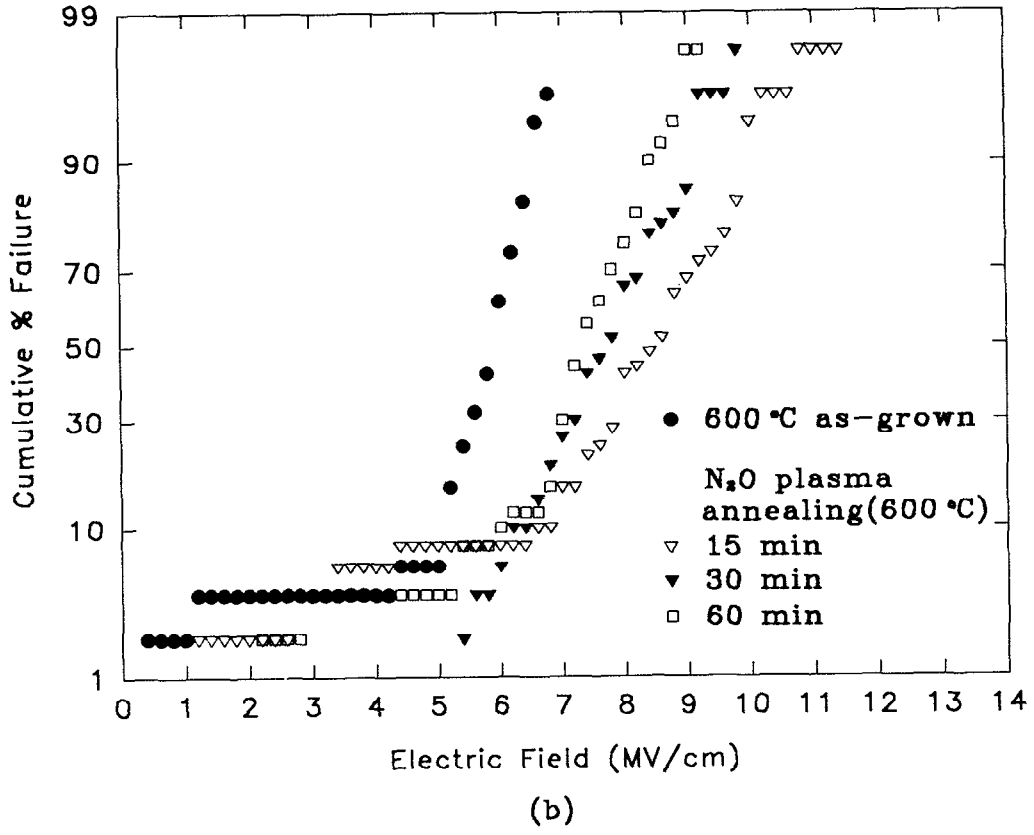

(b)

FIG. 4. (a) The breakdown-field distributions of the N_2O plasma-annealed oxides, (b) the cumulative failure rates of the 600 °C as-grown and N_2O plasma-annealed oxides.

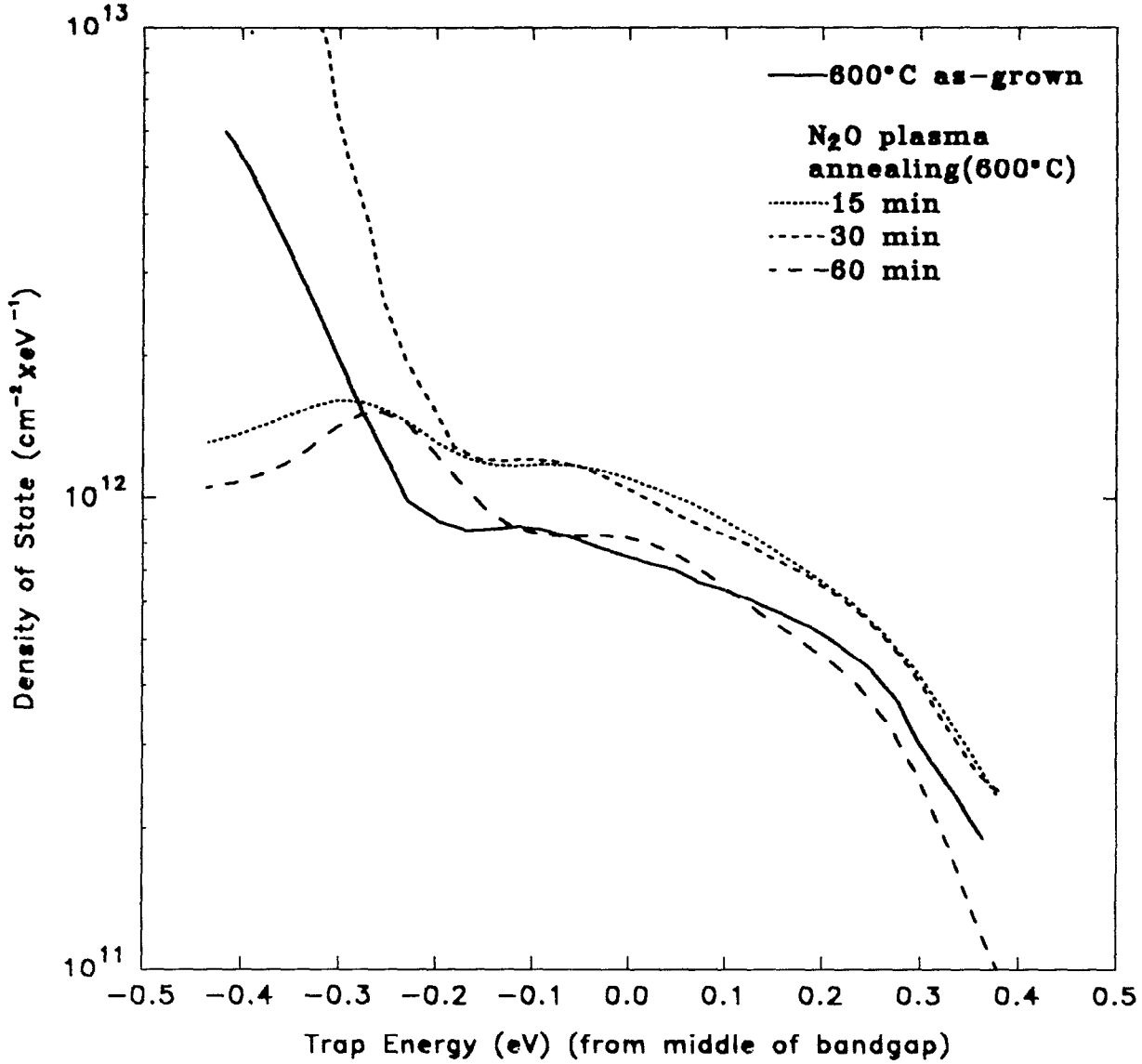

FIG. 5. The interface-state densities of the 600 °C as-grown and N_2O plasma-annealed oxides.

results of several NH_3 nitridation (annealing) processes.[32–34] It is attributed to nitrogen incorporation and production of interfacial stress-relaxation-induced defects;[35] however, the quantity of additional positive charges appears to be independent of the annealing time in this study. It is different from the time-dependent property of other nitridation techniques.[32–34] Furthermore, the Q_{eff} in N_2O plasma-annealed samples is also higher than that of the fluorinated oxides.

Figure 4(a) shows the breakdown-field distributions of the N_2O plasma-annealed oxides. The highest breakdown field of the 15 min N_2O plasma-annealed oxide was 12 MV/cm; however, the distribution was more dispersive than the 30 and 60 min annealed oxides. The N_2O plasma annealing indeed enhanced the oxide breakdown field above that of the as-grown oxide shown in Fig. 2(a). This result is clear from a comparison of the cumulative failure rate of these oxides, as shown in Fig. 4(b). As the electric field >7 MV/cm, the 600 °C as-grown oxides almost all failed (>90%), but the 15 min annealed oxide only had a 20% failure, and the 30 and 60 min annealed oxides failure rates were about 28%–30%. For higher electric field (>8 MV/cm), the failure rates depended on the N_2O plasma annealing time and are more easily to be distinguished. When the annealing time was longer, the failure rate of thin oxides at the specific field was higher.

Experimental results indicated that too much nitrogen incorporated in the oxides creates some defective sites during the longer annealing time.[36] Figure 5 illustrates the interface state density of N_2O plasma-annealed oxides. The D_{it} near the valence band of the oxide annealed for 15 min was lower than that of the as-grown oxide, but the D_{itm} was higher, and the D_{it} near the valence band was much increased after the 30 min N_2O plasma anneal. When the annealing time was prolonged to 60 min the D_{it} became low again, but D_{itm} was still the same as that of the as-grown oxide. So, it seems that N_2O plasma is more effective in annealing the D_{it} near the valence band. This annealing

mechanism may be similar to the fluorinated cases. The interfacial Si disordered layers and weak bonds could be annealed by N incorporation; however, Si dangling bonds at the interface may be produced and thereby result in a higher D_{itm}. As deduced from this annealing trend, a longer N_2O plasma annealing time (probably 2 h) might be required to anneal the interface-state density to a lower value. This tendency was also observed in a NH_3 rapid thermal nitridation experiment published previously.[32] Furthermore, this same tendency can be accounted for by the model proposed in Ref. 34 where the nitrogen incorporation would induce a defective state at first and later reduce the existing defective state by healing the strain.

IV. CONCLUSIONS

An investigation has been made for the first time of the inherent electrical properties of the as-grown, fluorinated, and N_2O plasma-annealed ultrathin oxides (7–8 nm) grown by 100 W microwave afterglow oxidation at low temperatures (400 and 600 °C). Higher forward microwave power might reduce the oxidation temperature, increase the oxidation rate, and further improve the oxide qualities; however, the fluorine and nitrogen introduced additional positive charges into the thin oxides. The fluorinated process at 600 °C could improve the oxide breakdown property as well as reduce the interface trap density. The oxide grown at 600 °C with a 15 min N_2O plasma annealing process provided the best oxide breakdown property (≈12 MV/cm) among the samples. Based on our data, the interface traps may be annealed to a lower value with a longer N_2O plasma annealing time (>1 h). These findings are similar to other fluorination and N_2O annealing results; however, the temperature employed was significantly lower in our work.

[1] J. Siejka and J. Perriere, Phys. Thin Films **14**, 81 (1989).
[2] C. Y. Fu, J. C. Mikkelsen, Jr., J. Schmitt, J. Abelson, J. C. Knights, N. Johnson, A. Barker, and M. J. Thompson, J. Electron. Mater. **14**, 685 (1985).
[3] T. Sugano, Mater. Res. Soc. Symp. Proc. **38**, 487 (1985).
[4] J. Seijka and J. Perrier, Mater. Res. Soc. Symp. Proc. **38**, 427 (1985).
[5] J. M. Cook, Solid State Technol. **April**, 147 (1987).
[6] J. Ruzyllo, A. Hoff, and G. Ruggles, J. Electron. Mater. **16**, 373 (1987).
[7] Y. Yasuda, S. Zaima, T. Kaida, and Y. Koide, Appl. Sur. Sci. **41/42**, 429 (1989).
[8] M. Tsuji, M. Sakumoto, and Y. Fujii, Chem. Lett. **1990**, 881.
[9] C. Vinkier, P. Coeckelberghs, G. Stevens, M. Heyns, and S. De Jaegere, J. Appl. Phys. **62**, 1450 (1987).
[10] Y. Yasuda, S. Zaima, T. Kaida, and Y. Koide, J. Appl. Phys. **67**, 2603 (1990).
[11] Y. Nishioka, E. F. da Silva, Jr., Y. Wang, and T. P. Ma, IEEE Electron Device Lett. **EDL-9**, 38 (1988).
[12] P. J. Wright and K. C. Sarawat, IEEE Trans. Electron Devices **ED-36**, 879 (1989).
[13] P. J. Wright, N. Kasai, S. Inoue, and K. Sarawat, IEEE Electron Device Lett. **EDL-10**, 347 (1989).
[14] W. Ting, G. Q. Lo, T. Y. Hsieh, D. L. Kwong, J. Kuehne, and C. W. Maegee, Appl. Phys. Lett. **56**, 2255 (1990).
[15] A. Uhiyama, H. Fukuda, T. Hayashi, T. Iwabushe, and S. Ohno, IEDM Tech. Dig. **1990**, 425.
[16] H. Hwang, W. Ting, D. L. Kwong, and J. Lee, IEDM Tech. Dig. **1990**, 421.
[17] J. Ahn, W. Ting, and D. L. Kwong, IEEE Electron Device Lett. **EDL-13**, 117 (1992).
[18] Z. Liu, H. Wann, P. K. Ko, C. Hu, and Y. C. Cheng, IEEE Electron Device Lett. **EDL-13**, 519 (1992).
[19] B. McCarroll, Rev. Sci. Instrum. **41**, 279 (1970).
[20] M. Meuris, S. Verhaverbeke, P. W. Mertens, M. M. Heyns, L. Hellemans, Y. Bruynseraede, and A. Philipossian, Jpn. J. Appl. Phys. (pt. 2) **31**, L1514 (1992).
[21] *Ionizing Radiation Effects in MOS Devices and Circuits*, edited by T. P. Ma and P. Dressendorfer (Wiley, New York, 1989).
[22] D. K. Schroder, *Semiconductor Material and Device Characterization* (Wiley, Singapore, 1990), Chap. 6.
[23] E. H. Nicollian and J. R. Brews, *MOS (Metal-Oxide-Semiconductor) Physics and Technology* (Wiley, New York, 1982), Chap. 15.
[24] G. Q. Lo, W. Ting, J. H. Ahn, D. L. Kwang, and J. Kuehne, IEEE Trans. Electron Devices **ED-39**, 148 (1992).
[25] K. Yamabe and K. Taniguchi, IEEE Trans. Electron Devices **ED-32**, 423 (1985).
[26] T. P. Ma, J. Vac. Sci. Technol. A **10**, 705 (1992).
[27] S.-P. Jeng, T.-P. Ma, R. Canteri, M. Anderle, and G. W. Rubloff, Appl. Phys. Lett. **61**, 1310 (1992).
[28] J. Singh and A. Madhukar, Appl. Phys. Lett. **38**, 884 (1981).
[29] T. Sakurai and T. Sugano, J. Appl. Phys. **52**, 2889 (1981).
[30] S. M. Sze, *Physics of Semiconductor Devices*, 2nd ed. (Wiley, Singapore, 1981), Chap. 7.
[31] J. Batey, E. Tierney, and T. N. Nguyen, IEEE Electron Device Lett. **EDL-8**, 148 (1987).
[32] T. Hori, Y. Naito, H. Iwasaki, and H. Esaki, IEEE Electron Device Lett. **EDL-7**, 669 (1986).
[33] D. K. Shih, W. T. Chang, S. K. Lee, Y. H. Ku, D. L. Kwong, and S. Lee, Appl. Phys. Lett. **52**, 1698 (1988).
[34] R. Koba and R. E. Tressler, J. Electrochem. Soc. **135**, 144 (1988).
[35] Y. Naito, T. Hori, H. Iwasaki, and H. Esaki, J. Vac. Sci. Technol. B **5**, 633 (1987).
[36] R. P. Vasquez and A. Madhukar, Appl. Phys. Lett. **47**, 998 (1985).